

1 **Siberian tree-ring and stable isotope proxies as indicators of temperature and moisture**
2 **changes after major stratospheric volcanic eruptions**

3

4 Olga V. Churakova^{1,2*}, Marina V. Fonti², Matthias Saurer^{3,4}, Sébastien Guillet¹, Christophe
5 Corona⁵, Patrick Fonti³, Vladimir S. Myglan⁶, Alexander V. Kirilyanov^{2,7,8}, Oksana V.
6 Naumova⁶, Dmitriy V. Ovchinnikov⁷, Alexander Shashkin^{2,7}, Irina Panyushkina⁹, Ulf
7 Büntgen^{3,8}, Malcolm K. Hughes⁹, Eugene A. Vaganov^{2,7,10}, Rolf T.W. Siegwolf^{3,4}, Markus
8 Stoffel^{1,11,12}

9 *¹Institute for Environmental Sciences, University of Geneva, CH-1205 Geneva, Switzerland*

10 *²Institute of Ecology and Geography, Siberian Federal University RU-660049 Krasnoyarsk,
11 Svobodny pr 79/10, Russia*

12 *³Swiss Federal Institute for Forest, Snow and Landscape Research WSL, Zürcherstrasse 111,
13 CH-8903 Birmensdorf, Switzerland*

14 *⁴Paul Scherrer Institute, CH- 5232 Villigen - PSI, Switzerland*

15 *⁵Université Blaise Pascal, Geolab, UMR 6042 CNRS, 4 rue Ledru, F-63057 Clermont-Fer-
16 rand, France*

17 *⁶Institute of Humanities, Siberian Federal University RU-660049 Krasnoyarsk, Svobodny pr
18 82, Russia*

19 *⁷Sukachev Institute of Forest SB RAS, Federal Research Center “Krasnoyarsk Science Cen-
20 ter SB RAS” RU-660036 Krasnoyarsk, Akademgorodok 50, bld. 28, Russia*

21 *⁸Department of Geography, University of Cambridge, Downing Place, Cambridge CB2 3EN*

22 *⁹Laboratory of Tree-Ring Research, University of Arizona, 1215 E. Lowell St., Tucson, 85721,
23 USA*

24 *¹⁰Siberian Federal University, Rectorate, RU-660049 Krasnoyarsk, Svobodny pr 79/10, Rus-
25 sia*

26 ¹¹*dendrolab.ch, Department of Earth Sciences, University of Geneva, 13 rue des Maraîchers,*
27 *CH-1205 Geneva, Switzerland*

28 ¹²*Department F.A. Forel for Aquatic and Environmental Sciences, University of Geneva, 66*
29 *Boulevard Carl-Vogt, CH-1205 Geneva, Switzerland*

30

31 **Corresponding author:** Olga V. Churakova*

32 E-Mail: olga.churakova@hotmail.com

33

34

35

36

37

38

39

40

41

42

43

44

45

46 **Abstract**

47 Stratospheric volcanic eruptions have far-reaching impacts on global climate and society. Tree
48 rings can provide valuable climatic information on these impacts across different spatial and
49 temporal scales. Here we explore the suitability of tree-ring width (TRW), maximum latewood
50 density (MXD), cell wall thickness (CWT), and $\delta^{13}\text{C}$ and $\delta^{18}\text{O}$ in tree-ring cellulose for the
51 detection of climatic changes after the six major volcanic eruptions in the high-latitude and
52 high-altitude Siberian regions. Conifer trees from these regions are highly sensitive to climatic
53 changes and may be considered as key regions for studying extreme climatic events. We study the impact
54 of the six stratospheric volcanic eruptions (535, 540, 1257, 1640, 1815 and 1991) on larch trees
55 from three Siberian regions: northeastern Yakutia - YAK, eastern Taimyr - TAY and Russian
56 Altai - ALT, sites located within 1500-2000 km away from each other.

57 Our findings suggest that TRW, MXD, and CWT show strong summer air temperature anomalies
58 in 536, 541-542, and 1258-1259 at all study sites. However, no further extreme hydro-
59 climatic anomalies occurred at Siberian sites after the volcanic eruptions 1640, 1815 and 1991.
60 Based on $\delta^{13}\text{C}$ data, 536 was extremely humid in YAK and TAY, whereas 541 was humid in
61 ALT. In contrast, the 1257 eruption of Samalas likely led to at least two dry summers across
62 two Siberian sites. Summer sunshine duration decreased significantly in 536, 541-542, 1258-
63 1259 in YAK, and 536 in ALT. We show that trees growing at YAK and ALT responded
64 mainly during the first year after the eruptions, whereas a two-year delay occurs at TAY.
65 Since climatic responses to selected stratospheric volcanic eruptions are different, and thus
66 affect ecosystem functioning and productivity differently in space and time, a combined as-
67 sessment of multiple tree-ring parameters and large number of samples from Siberian sites is
68 needed to provide a more complete picture of past climate dynamics, which in turn appears
69 fundamental to validate global climate models.

70

71 **Key words:** $\delta^{13}\text{C}$ and $\delta^{18}\text{O}$ in tree-ring cellulose, tree-ring width, maximum latewood den-
72 sity, cell wall thickness, drought, temperature, precipitation, sunshine duration, vapor pres-
73 sure deficit

74

75 **1. Introduction**

76 Major stratospheric volcanic eruptions can substantially modify the Earth's radiative balance
77 and cool the troposphere. This is due to the massive injection of sulphate aerosols, which are
78 able to reduce surface temperatures on timescales ranging from months to years (Robock,
79 2000). **The cooling** associated with the radiative effects of volcanic aerosols, which absorb
80 terrestrial radiation and scatter incoming solar radiation significantly, has been estimated to
81 about 0.5°C during the two years following the Mount Pinatubo eruption in June 1991 (Hansen
82 et al., 1996).

83 Since trees – as living organisms – are impacted in their metabolism by environmental changes,
84 their responses to these changes are recorded in the biomass, as it is found in tree-ring param-
85 eters (Schweingruber, 1996). The decoding of tree-ring archives therefore is used to reconstruct
86 past climates. A summer cooling of the Northern Hemisphere (NH) ranging from 0.6°C to
87 1.3°C has been reported after the strongest eruptions of the past 1,500 years: CE 1257 Samalas,
88 1452/3 Unknown, 1600 Huaynaputina, and 1815 Tambora eruptions based on tree-ring width
89 (TRW) and maximum latewood density (MXD) reconstructions (Briffa et al., 1998; Schneider
90 et al., 2015; Stoffel et al., 2015; Wilson et al., 2016; Esper et al., 2017; Guillet et al., 2017).

91 According to climate simulations, significant changes in the precipitation regime can also be
92 expected after large volcanic eruptions; these include, among others, rainfall deficit in monsoon
93 prone regions and in Southern Europe (Joseph and Zeng, 2011) as well as wetter than normal
94 conditions in Northern Europe (Robock and Liu 1994; Gillet et al., 2004; Peng et al., 2009;

95 Meronen et al., 2012; Iles et al., 2013; Wegmann et al., 2014). However, despite recent ad-
96 vances in the field, the impacts of stratospheric volcanic eruptions on the hydro-climatic vari-
97 ability at regional scales remain largely unknown. Therefore, this relevant knowledge about
98 moisture anomalies is critically needed, especially at high-latitude sites where tree growth is
99 mainly limited by summer temperatures.

100 As dust and aerosol particles of large volcanic eruptions affect primarily the radiation regime,
101 three major drivers of plant growth, i.e. photosynthetic active radiation (PaR), temperature and
102 vapor pressure deficit (VPD) will be affected by volcanic activity. This is reflected in reduced
103 TRW as a result of reduced photosynthesis but even more so by low temperature. As cell divi-
104 sion is also temperature dependent, its rate (tree-ring growth) will exponentially decrease with
105 decreasing temperature below +3°C (Körner, 2015), outweighing the “low light / low-photo-
106 synthesis” effect by far.

107 Furthermore, over the last years, some studies using mainly carbon isotopic signals ($\delta^{13}\text{C}$) in
108 tree rings showed eco-physiological responses of trees to volcanic eruptions at mid- (Bat-
109 tipaglia et al., 2007) or high- (Gennaretti et al., 2017) latitudes. By contrast, a combination of
110 both carbon ($\delta^{13}\text{C}$) and oxygen ($\delta^{18}\text{O}$) isotopes in tree rings has been employed only rarely to
111 trace CE volcanic eruptions in high-latitude or high-altitude proxy records (Churakova (Si-
112 dorova) et al., 2014).

113 Approaches including TRW, MXD and cell wall thickness (CWT) as well as $\delta^{13}\text{C}$ and $\delta^{18}\text{O}$ in
114 tree cellulose are a promising way to disentangle hydro-climatic variability as well as winter
115 and early spring temperatures at high-latitude and high-altitude sites (Sidorova et al., 2008,
116 2010, 2011; Churakova (Sidorova) et al., 2014). In that sense, recent work has allowed the
117 retrieval of high-resolution, seasonal information on water and carbon limitations on growth
118 during spring and summer from CWT measurements (Panyushkina et al., 2003; Sidorova et
119 al., 2011; Fonti et al., 2013; Bryukhanova et al., 2015). Depending on site conditions, $\delta^{13}\text{C}$

120 variations reflect light (stand density) (Loader et al., 2013), water availability (soil properties)
121 and air humidity (proximity to open waters, i.e. rivers, lakes, swamps and orography) as these
122 parameters have been recognized to modulate the stomatal conductance (g) controlling carbon
123 isotopic discrimination.

124 Depending on the study site, a decrease in the carbon isotope ratio can be expected after strat-
125 ospheric volcanic eruptions due to limited photosynthetic activity and higher stomatal conduct-
126 ance, which in turn would be the result of decreased temperatures, VPD and a reduction in light
127 intensity. By contrast, volcanic eruptions have also been credited for an increase in photosyn-
128 thesis as dust and aerosol particles cause an increased light scattering, compensating for the
129 light reduction (Gu et al., 2003). A significant increase in $\delta^{13}\text{C}$ values in tree-ring cellulose
130 should be interpreted as an indicator of drought (stomatal closure) or high photosynthesis (Far-
131 quhar et al., 1982).

132 In the past, very limited attention has been given to the elemental and isotopic composition of
133 tree rings in years during which they may have been subjected to the climatic influence of
134 powerful, but remote, and often tropical, volcanic eruptions.

135 In this study, we aim to fill this gap by investigating the response of different components of
136 the Siberian climate system (i.e. temperature, precipitations, VPD, and sunshine duration) to
137 the largest volcanic events of the last 1,500 years. By doing so, we seek to extend our under-
138 standing of the effects of volcanic eruptions on climate by combining multiple climate sensitive
139 variables measured in tree rings that were formed around the time of the major volcanic erup-
140 tions (see Table 1). We focus our investigation on remote, two high-latitude (northeastern Ya-
141 kutia), YAK and eastern Taimyr (TAY) and one high-altitude (Russian Altai, ALT) Siberian
142 sites, where long tree-ring chronologies with high climate sensitivity exist. Therefore, we de-
143 veloped a dataset including five tree-ring proxies: TRW, MXD, CWT, $\delta^{13}\text{C}$ and $\delta^{18}\text{O}$ stable
144 isotope chronologies derived from larch trees to (1) determine the major climatic drivers of the

145 above mentioned proxies and to evaluate their suitability in terms of climate responsiveness,
146 for each proxy separately and in combination; and (2) based on these analyses reconstruct the
147 climatic effect of these unusually large CE volcanic eruptions (Table 1).

148

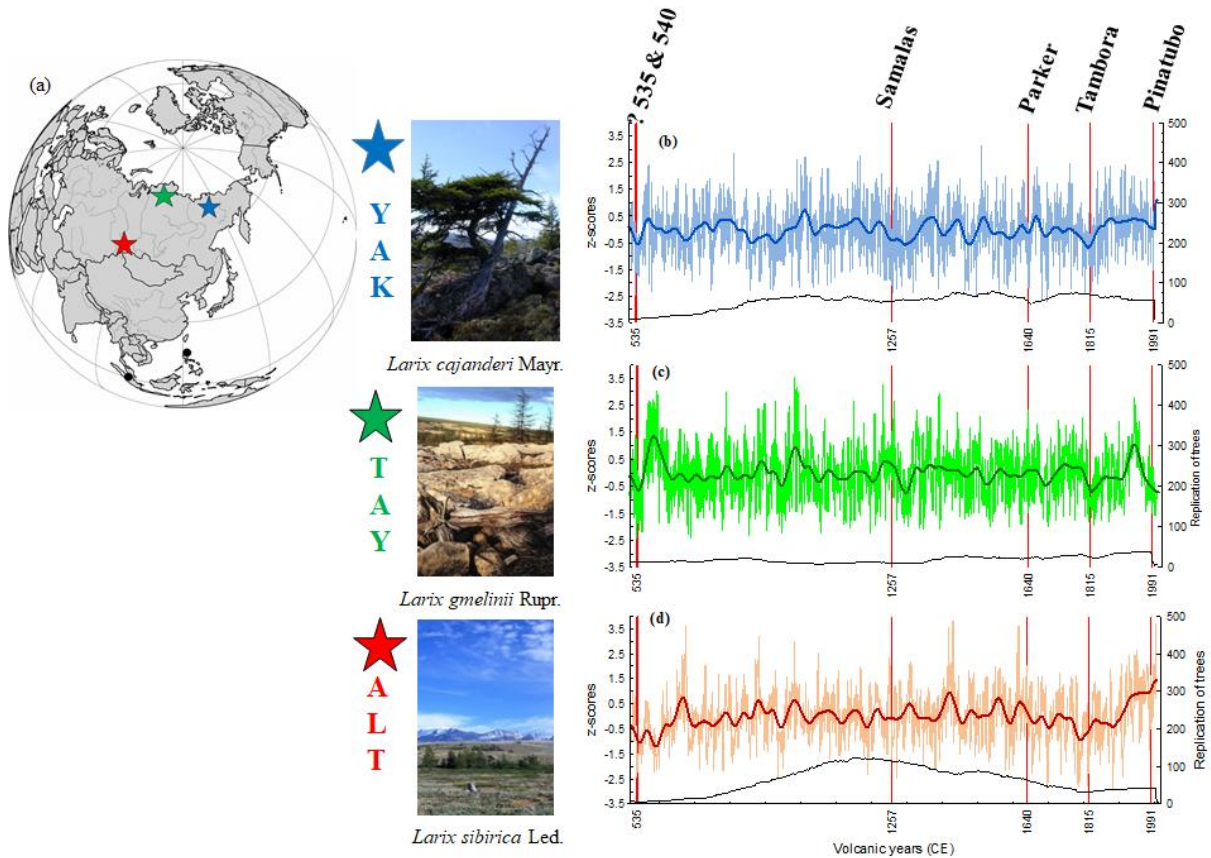
149 **2. Material and methods**

150

151 *2.1. Study sites*

152 The study sites are situated in Siberia (Russian Federation), far away from industrial centers,
153 in zones characterized by continuous permafrost in northeastern Yakutia (YAK, 69°N, 148°E);
154 eastern Taimyr (TAY, 70°N, 103°E) and in the Altai mountains (ALT, 50°N, 89°E) (Fig. 1a,
155 Table 2). Tree-ring samples were collected during several expeditions and included old relict
156 wood and living larch trees, *Larix cajanderi* Mayr (max. 1216 years) in YAK, *Larix gmelinii*
157 Rupr. (max. 640 years) in TAY and *Larix sibirica* Ldb. (max. 950 years) in ALT. TRW chro-
158 nologies have been developed and published in the past (Fig. 1, Hughes et al., 1999; Sidorova
159 and Naurzbaev 2002; Sidorova 2003 for YAK; Naurzbaev et al., 2002 for TAY; Myglan et al.,
160 2008 for ALT).

161 Mean annual air temperature is lower at the high-latitude YAK and TAY sites than at the high-
162 altitude ALT site (Table 2). Annual precipitation totals are very low for all study sites. The
163 vegetation period calculated with a growth threshold of +5°C (Fritts 1976; Schweingruber
164 1996) is very short (50-120 days) at all locations (Table 2). Sunshine duration for tree growth
165 is higher at YAK and TAY (ca. 18-20 h/day in summer) compared to ALT (ca. 18 h/day in
166 summer) (Sidorova et al., 2005; Myglan et al., 2008; Sidorova et al., 2011; Churakova (Si-
167 dorova) et al., 2014).



168
 169 **Fig. 1.** Map with the locations of the study sites (stars) and volcanic eruptions from the tropics
 170 (black dots) considered in this study (a). Annual tree-ring width index (light lines) and
 171 smoothed by 51-year Hamming window (bold lines) chronologies from northeastern Yakutia
 172 (YAK - blue, b) (Hughes et al., 1999; Sidorova and Naurzbaev 2002; Sidorova 2003), eastern
 173 Taimyr (TAY - green, c) (Naurzbaev et al., 2002), and Russian Altai (ALT - red, d) (Myglan
 174 et al., 2009) were constructed based on larch trees (Photos: V. Myglan – ALT, M. M.
 175 Naurzbaev – YAK, TAY).

176
 177 *2.2. Selection of the study periods and larch subsamples*

178 Volcanic aerosols deposited in ice core records (Gao et al., 2008; Crowley and Untermann,
 179 2013; Sigl et al., 2015; Toohey and Sigl 2017) **attest to 6 strong volcanic eruptions** in CE 535,
 180 540, 1257, 1640, 1815, and 1991, that may have had a noticeable impact on the climate system.

181 Therefore, our selection was based on the literature review (Table 1) and 5 available tree-ring
182 proxies covering the specific periods, characterized by volcanic eruptions.

183

184 To investigate climatic impacts of these eruptions in Siberian regions we developed MXD,
185 CWT, $\delta^{13}\text{C}$ and $\delta^{18}\text{O}$ chronologies for the following periods around (± 10 years): CE 525-545,
186 1247-1267, 1630-1650, 1805-1825, and 1950-2000, with the latter being used to calibrate tree-
187 ring proxy versus available climate data (Table 2).

188 Material was prepared from the 2000-yr long TRW chronologies available at each of the sites
189 from the previous studies (Fig. 1 b-d). According to the level of conservation of the material,
190 the largest possible number of samples was prepared for each of the proxies. Unlike TRW,
191 which could be measured on virtually all samples, some of the material was not available with
192 sufficient quality to allow for tree-ring anatomy and stable isotope analysis. We therefore use
193 a smaller sample size for CWT (n=4) and stable isotopes (n=4) than for TRW (n=12) or MXD
194 (n=12). Nonetheless, replications are still comparable with those used in reference papers in
195 the fields of CWT and isotope analyses (Loader et al., 1997; Panyushkina et al., 2003; Fonti et
196 al., 2013).

197

198

199

200 **Table 1.** List of stratospheric volcanic eruptions used in the study.

Study period (CE)	Date of eruption Month/Day/Year	Volcano name	Volcanic Explosivity Index (VEI)	Location, coordinates	References
525-545	NA/NA/535	Unknown	?	Unknown	Stothers, 1984
	NA/NA/540	Unknown	?	Unknown	Sigl et al., 2015; Toohey, Sigl 2017
1247-1267	May-October/NA/ 1257	Samalas	7	Indonesia, 8.42°N, 116.47°E	Lavigne et al., 2013; Stothers, 2000; Sigl et al., 2015
1630-1650	December/26/1640	Parker	5	Philippines, 6°N, 124°E	Zielinski et al., 1994
1805-1825	April/10/1815	Tambora	7	Indonesia, 8°S, 118°E	Zielinski et al., 1994
1950 - 2000	June/15/1991	Pinatubo	6	Philippines, 15°N, 120°E	Zielinski et al., 1994; Sigl et al., 2015

201 NA – not available.

202

203

204

205

206 **Table 2.** Summary of tree-ring sites in northeastern Yakutia (YAK), eastern Taimyr (TAY), and Altai (ALT) and weather stations used in the
 207 study. Monthly air temperature (T, °C), precipitation (P, mm), sunshine duration (S, h/month) and vapor pressure deficit (VPD, kPa) data were
 208 used from the available meteorological database: <http://aisori.meteo.ru/ClimateR>.

Site	Species	Location	Weather station	Meteorological parameters				Length of vegetation period (day)	Thawing permafrost depth (max, cm)	Annual air temperature (°C)	Annual precipitation (mm)
				T (°C)	P (mm)	S (h/month)	VPD (kPa)				
				Periods							
YAK	<i>Larix cajanderi</i> Mayr.	69°N, 148°E	Chokurdach 62°N, 147°E, 61 m. a.s.l.	1950-2000	1966-2000	1961-2000	1950-2000	50-70*	20-50*	-14.7	205
TAY	<i>Larix gmelinii</i> Rupr.	70°N, 103°E	Khatanga 71°N, 102°E, 33m. a.s.l.	1950-2000	1966-2000	1961-2000	1950-2000	90**	40-60**	-13.2	269
ALT	<i>Larix sibirica</i> Ledeb.	50°N, 89°E	Mugur Aksy 50°N, 90°E 1850 m. a.s.l.	1963-2000	1966-2000			90-120***	80-100***	-2.7	153
			Kosh-Agach 50°N, 88°E 1758 m.a.s.l.			1961-2000	1950-2000				

209 *Abaimov, 1996; Hughes et al., 1999; Churakova (Sidorova) et al., 2016

210 **Naurzbaev et al., 2002

211 ***Sidorova et al., 2011

212 *2.3. Tree-ring width analysis*

213 Ring width of 12 trees was re-measured for each selected period. Cross-dating was checked by
214 comparison with the existing complete 2000-yr TRW chronologies (Fig. 1). The TRW series were
215 standardized using the ARSTAN program (Cook and Krusic, 2008) based on the negative expo-
216 nential curve ($k > 0$) or a linear regression (any slope) prior to averaging with the bi-weight robust
217 mean (Cook and Kairiukstis 1990). Signal strength in regional TRW chronologies was assessed
218 with the Expressed Population Signal (EPS) statistics as it measures how well the finite sample
219 chronology compares with a theoretical population chronology based on an infinite number of
220 trees (Wigley et al., 1984). RBAR and EPS values of stable isotope chronologies were calculated
221 for the period from 1950 to 2000, for which individual trees were analyzed separately, and show
222 the common signal with an $EPS > 0.85$. Back in time, we used pooled material only. For all other
223 tree-ring parameters, EPS also exceeds the threshold of 0.85.

224

225 *2.4. Image analysis of cell wall thickness (CWT)*

226 Analysis of wood anatomical features was performed for all studied periods with an AxioVision
227 scanner (Carl Zeiss, Germany). Micro-sections were prepared using a sliding microtome and
228 stained with methyl blue (Furst, 1979). Tracheids in each tree ring were measured along five radial
229 files of cells (Munro et al., 1996; Vaganov et al., 2006) selected for their larger tangential cell
230 diameter (T). For each tracheid, CWT and the radial cell diameter (D) were computed. In a second
231 step, tracheid anatomical parameters were averaged for every tree ring. Site chronologies are pre-
232 sented for the complete annual ring chronology without standardization due to the absence of low-
233 frequency trend. CWT data from ALT for the periods 1790-1835 and 1950-2000 were used from
234 the past studies (Sidorova et al., 2011; Fonti et al., 2013) and for YAK for the period from 1600-
235 1980 from Panyushkina et al. (2003). Unfortunately the remaining sample material for the CE 536
236 ring at TAY was insufficient to produce a clear anatomical signal. As a result, CWT is missing for
237 CE 536 at TAY (Fig. 2).

238 2.5. *Maximum latewood density (MXD)*

239 Maximum latewood density chronologies from ALT were available continuously for the period
 240 CE 1407-2007 from Schneider et al. (2015) and for YAK and TAY the period CE 1790-2004 from
 241 Sidorova et al. (2010). For any of the other periods, at least six cross-sections (for CE 516-560,
 242 only four sections could be used, as this period is not as well replicated) were sawn with a double-
 243 bladed saw, to a thickness of 1.2 mm, at right angles to the fiber direction. Samples were exposed
 244 to X-rays for 35-60 min (Schweingruber 1996). MXD measurements were obtained with a reso-
 245 lution of 0.01 mm, and brightness variations transferred into (g/cm^3) using a calibration wedge
 246 (Lenz et al., 1976; Eschbach et al., 1995) from a Walesch X-ray densitometer 2003. All MXD
 247 series were detrended in ARSTAN by calculating subtractions from straight-line functions (Fritts,
 248 1976). Site chronologies were developed for each volcanic period using the bi-weight robust mean.
 249

250 2.6. *Stable carbon ($\delta^{13}\text{C}$) and oxygen ($\delta^{18}\text{O}$) isotopes in tree-ring cellulose*

251 During photosynthetic CO_2 assimilation $^{13}\text{CO}_2$ is discriminated against $^{12}\text{CO}_2$, leaving the newly
 252 produced assimilates depleted in ^{13}C . The carbon isotope discrimination ($^{13}\Delta$) is partitioned in the
 253 diffusional component with $a = 4.4\text{‰}$ and the biochemical fractionation with $b = 27\text{‰}$, for C3
 254 plants, during carboxylation via Rubisco. The $^{13}\Delta$ is directly proportional to the c_i/c_a ratio, where
 255 c_i is the leaf intercellular, and c_a the ambient CO_2 concentration. This ratio reflects the balance
 256 between stomatal conductance (g_l) and photosynthetic rate (A_N). A decrease in g_l at a given A_N
 257 results in a decrease of $^{13}\Delta$, as c_i/c_a decreases and vice versa. The same is true when A_N increases
 258 or decreases at a given g_l . Since CO_2 and H_2O gas exchange are strongly interlinked with the C-
 259 isotope fractionation $^{13}\Delta$ is controlled by the same environmental variables i.e. PaR, CO_2 , VPD
 260 and temperature (Farquhar et al., 1982, 1989; Cernusak et al., 2013).

261 The oxygen isotopic compositions of tree-ring cellulose record the $\delta^{18}\text{O}$ of the source water de-
 262 rived from precipitation, which itself is related to temperature variations at middle and high lati-
 263 tudes (Craig, 1961; Daansgard, 1964). It is modulated by evaporation at the soil surface and to a

264 larger degree by evaporative and diffusion processes in leaves; the process is largely controlled by
265 the vapor pressure deficit (Dongmann et al., 1972, Farquhar and Lloyd, 1993, Cernusak et al.,
266 2016). A further step of fractionation occurs as sugar molecules are transferred to the locations of
267 growth (Roden et al., 2000). During the formation of organic compounds the biosynthetic frac-
268 tionation leads to a positive shift of the $\delta^{18}\text{O}$ values by 27‰ relative to the leaf water (Sternberg,
269 2009). The oxygen isotope variation in tree-ring cellulose therefore reflects a mixed climate infor-
270 mation, often dominated by a temperature, source water or sunshine duration modulated by the
271 VPD influence.

272 The cross-sections of relict wood and cores from living trees used for the TRW, MXD and CWT
273 measurements were then selected for the isotope analyses. We analyzed four subsamples for each
274 studied period according to the standards and criteria described in Loader et al. (2013). The first
275 50 yrs. of each sample were excluded to limit juvenile effects (McCarroll and Loader, 2004). After
276 splitting annual rings with a scalpel, the whole wood samples were enclosed in filter bags. α -
277 cellulose extraction was performed according to the method described by Boettger et al. (2007).
278 For the analyses of $^{13}\text{C}/^{12}\text{C}$ and $^{18}\text{O}/^{16}\text{O}$ isotope ratios, 0.2-0.3 mg and 0.5-0.6 mg of cellulose were
279 weighed for each annual ring, into tin and silver capsules, respectively. Carbon and oxygen iso-
280 topic ratios in cellulose were determined with an isotope ratio mass spectrometer (Delta-S, Finni-
281 gan MAT, Bremen, Germany) linked to two elemental analyzers (EA-1108, and EA-1110 Carlo
282 Erba, Italy) via a variable open split interface (CONFLO-II, Finnigan MAT, Bremen, Germany).
283 The $^{13}\text{C}/^{12}\text{C}$ ratio was determined separately by combustion under oxygen excess at a reactor tem-
284 perature of 1020°C. Samples for $^{18}\text{O}/^{16}\text{O}$ ratio measurements were pyrolyzed to CO at 1080°C
285 (Saurer et al., 1998). The instrument was operated in the continuous flow mode for both, the C and
286 O isotopes. The isotopic values were expressed in the delta notation multiplied by 1000 relative to
287 the international standards (Eq. 1):

$$288 \quad \delta \text{ sample} = R_{\text{sample}}/R_{\text{standard}}-1 \quad (\text{Eq. 1})$$

289 where R_{sample} is the molar fraction of $^{13}\text{C}/^{12}\text{C}$ or $^{18}\text{O}/^{16}\text{O}$ ratio of the sample and R_{standard} the molar
290 fraction of the standards, Vienna Pee Dee Belemnite (VPDB) for carbon and Vienna Standard
291 Mean Ocean Water (VSMOW) for oxygen. The precision is $\sigma \pm 0.1\%$ for carbon and $\sigma \pm 0.2\%$
292 for oxygen. To remove the atmospheric $\delta^{13}\text{C}$ trend after CE 1800 from the carbon isotope values
293 in tree rings (i.e. Suess effect, due to fossil fuel combustion) we used atmospheric $\delta^{13}\text{C}$ data from
294 Francey et al. (1999), <http://www.cmdl.noaa.gov./info/ftpdata.html>). These corrected series were
295 used for all statistical analyses. The $\delta^{18}\text{O}$ cellulose series were not detrended.

296

297 *2.7. Climatic data*

298 Meteorological series were obtained from local weather stations close to the study sites and used
299 for the computation of correlation functions between tree-ring proxies and monthly climatic pa-
300 rameters (Table 2). Sunshine duration data were obtained from available Kosh-Agach meteoro-
301 logical station (<http://aisori.meteo.ru/ClimateR>).

302

303 *2.8. Statistical analysis*

304 All chronologies for each period were normalized to z-scores (Fig. 2). To assess post-volcanic
305 climate variability, we used Superposed Epoch Analysis (SEA, Panofsky and Brier, 1958) with
306 the five proxy chronologies available at each of the three study sites. In this experiment, the 15
307 years before and after a volcanic eruption were analyzed. SEA is applied to the six annually dated
308 volcanic eruptions (Table 1).

309 To test the sensitivity of the studied tree-ring parameters to climate, bootstrap correlation functions
310 have been computed between proxy chronologies and monthly climate predictors using the
311 ‘bootRes’ package of R software (R Core Team 2016) for the period 1950 (1966)-2000.

312 To estimate whether volcanic years can be considered as extreme, we computed Probability Den-
313 sity Functions (PDFs, Stirzaker, 2003) for each study site and for each tree-ring parameter over a
314 period of 221 years for which measurements are available (Fig. S1). A year is considered (very)

315 extreme if the value of a given parameter is below the (5th) 10th percentile of the PDF. We applied
 316 unpaired t-test statistics to check significance between each proxy and each site.

317

318 3. Results

319 3.1. Anomalies in tree-ring proxy chronologies after stratospheric volcanic eruptions

320 Normalized TRW chronologies show negative deviations the year following the eruptions at all
 321 studied sites (Fig. 2). Regarding CWT, a strong decrease is observed in CE 536 at YAK and ALT.

322 Only two layers of cells were formed in CE 536 for YAK as compared to the 11-20 layers of cells
 323 formed on average during “normal” years. In addition, we also observe the formation of frost rings
 324 in ALT between CE 536 and 538, as well as in 1259.

325 Furthermore, we revealed decreasing MXD values for ALT (-4.4 σ) in CE 537 and YAK (-2.8 σ)

326 in CE 536. However, for TAY, we found less pronounced patterns of the MXD variation (Fig.

327 2). In this regard, the sharpest decrease was observed in the CWT chronologies from YAK (-

328 2.4 σ) in CE 540 compared to TAY and ALT (Fig. 2). ALT $\delta^{18}\text{O}$ chronology recorded drastic de-

329 crease in the year of 536 with (- 4.8 σ) (Fig. 2, Fig. S1). While, $\delta^{18}\text{O}$ decrease for YAK was

330 found after Samalos eruption in CE 1259 only. Opposite, to increased $\delta^{18}\text{O}$ values towards CE

331 1259 from ALT (Fig. 2).

332 Finally, $\delta^{13}\text{C}$ negative anomalies are observed in YAK and TAY, and – to a lesser extent – in ALT.

333 The CE 540 eruption was less pronounced recorded in tree-ring proxies from TAY, compared to

334 YAK and ALT (Fig. 2). With respect to the CE 1257 Samalas eruption (Fig. 2), the year following

335 the eruption was recorded as very extreme in the TRW, MXD, $\delta^{18}\text{O}$, while less extreme in CWT

336 and $\delta^{13}\text{C}$ chronologies from YAK. ALT chronologies show synchronous decrease for all proxies

337 with following two years after the eruption (see Fig. S1).

338

YAK

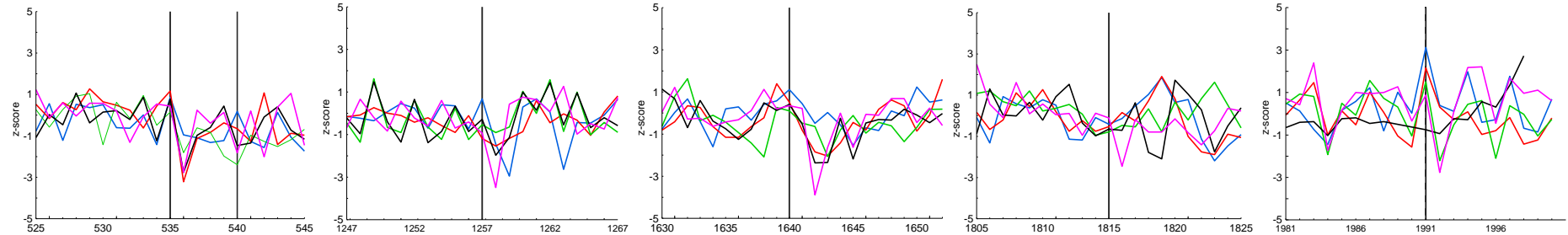
535 540

1257

1640

1815

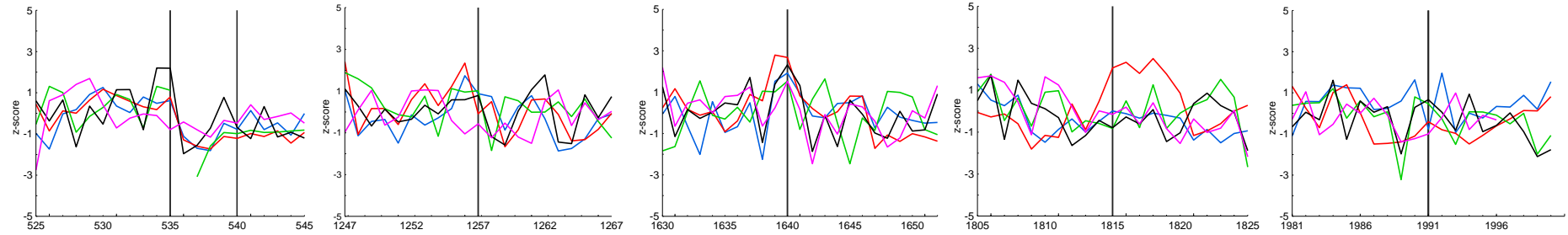
1991



339

340

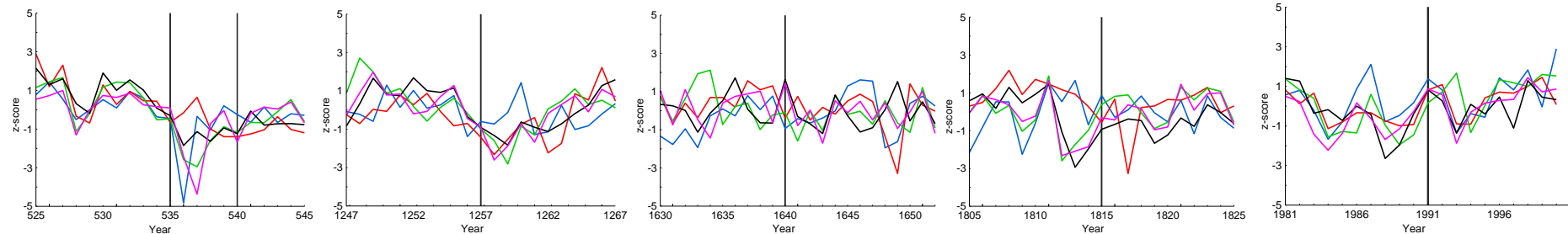
TAY



341

342

ALT



343

344

345 **Fig. 2.** Normalized (z-score) individual tree-ring index chronologies (TRWi, black), maximum latewood density (MXD, purple), cell wall thick-
 346 ness (CWT, green), $\delta^{13}\text{C}$ (red) and $\delta^{18}\text{O}$ (blue) in tree-ring cellulose chronologies from YAK, TAY and ALT for the specific periods 10 years
 347 before and after the eruptions CE 535, 1257, 1640, 1815 and 1991 are presented. Vertical lines showed year of the eruptions.

348

349 The impacts of the more recent CE 1640 Parker, 1815 Tambora, and 1991 Pinatubo eruptions
350 are, by contrast, far less obvious. In CE 1642, decreases of values are observed in all tree-ring
351 proxies from high-latitude sites YAK and TAY, whereas tree-ring proxies are not clearly af-
352 fected at ALT (mainly for the TRW and MXD, less for $\delta^{13}\text{C}$ and $\delta^{18}\text{O}$).

353 No extreme anomalies are observed in CE 1816 in Siberia regardless of the site and the tree-
354 ring parameter analyzed. The ALT $\delta^{13}\text{C}$ in CE 1817 and YAK MXD in 1816 can be seen as an
355 exception to the rule here as it evidenced extreme values, respectively.

356 Finally, the Pinatubo eruption is captured in CE 1992 mainly by MXD and CWT chronologies
357 from YAK. Simultaneous decrease of all tree-ring proxies from ALT is observed in 1993 (Fig.
358 2, S1), however, cannot be classified as extreme.

359 Overall, the SEA (Fig. 3) shows the high spatiotemporal variability and complexity of the re-
360 sponse of the Siberian climate system to the largest volcanic events over past millennium (CE
361 535, 540, 1257, 1641, 1815 and 1991). A short-term response by two years after the eruptions
362 is observed in the CWT proxies for TAY, while for YAK and ALT the CWT decrease lasts
363 longer (up to 5-6 years in ALT and YAK, respectively) (Fig. 3). The behavior of isotope chro-
364 nologies is rather more complex, with a distinct decrease in $\delta^{13}\text{C}$ at the high-latitude sites (YAK,
365 TAY), whereas $\delta^{18}\text{O}$ series are impacted mainly at the high-latitude YAK and high-altitude ALT
366 sites. We find significant differences ($p=0.014$, $df=40$, $n=21$) between averaged $\delta^{13}\text{C}$ chronol-
367 ogies of the YAK and ALT sites. SEA for TRW and MXD show a more drastic decrease of
368 values during the first year, mainly for TRW from YAK, and MXD from ALT when compared
369 to other proxies and study sites (Fig. 3).

370

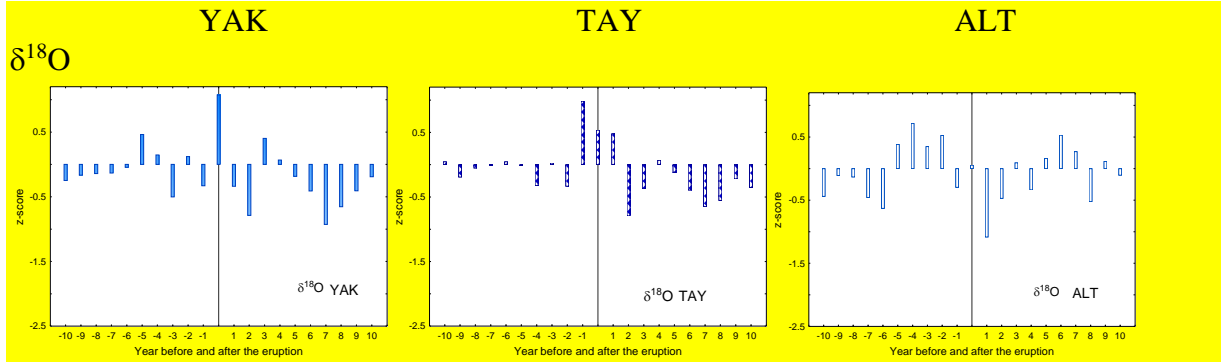
371

372

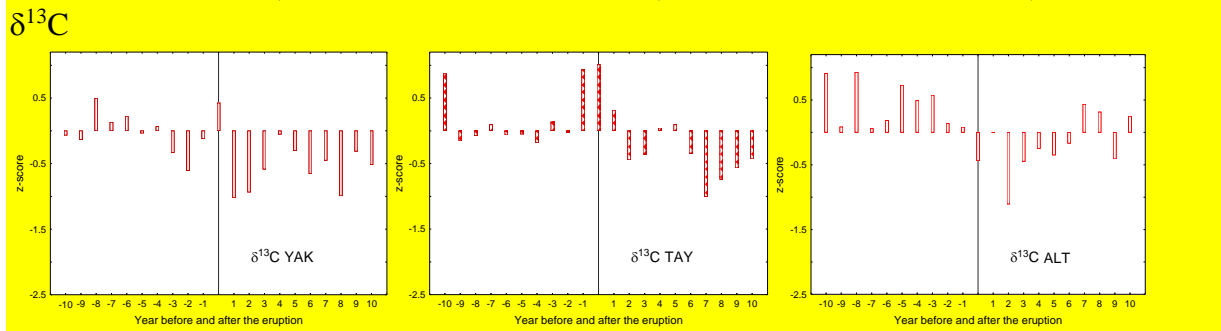
373

SIBERIAN TREES AND VOLCANIC ERUPTIONS

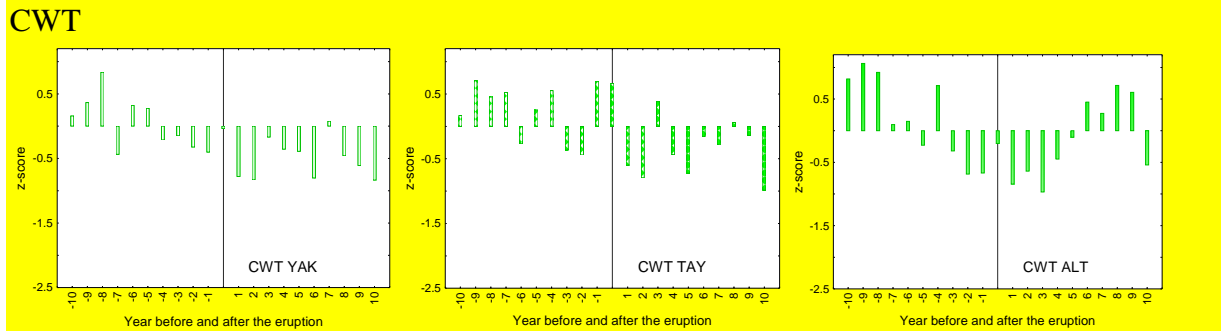
374
375



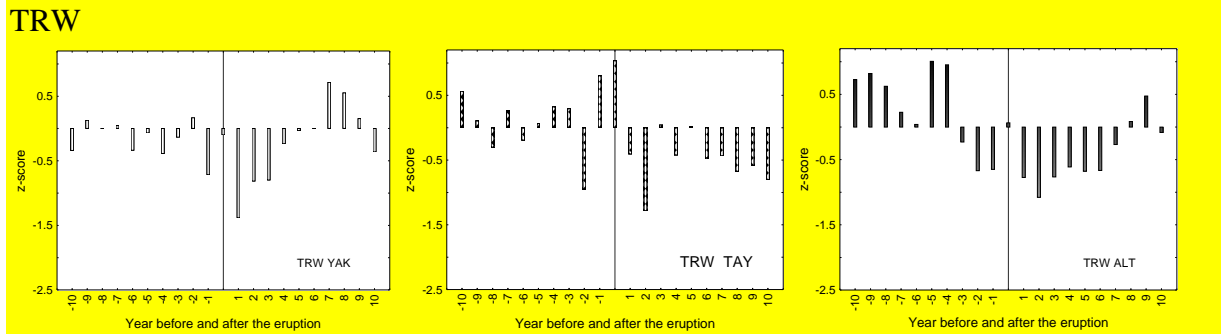
376
377



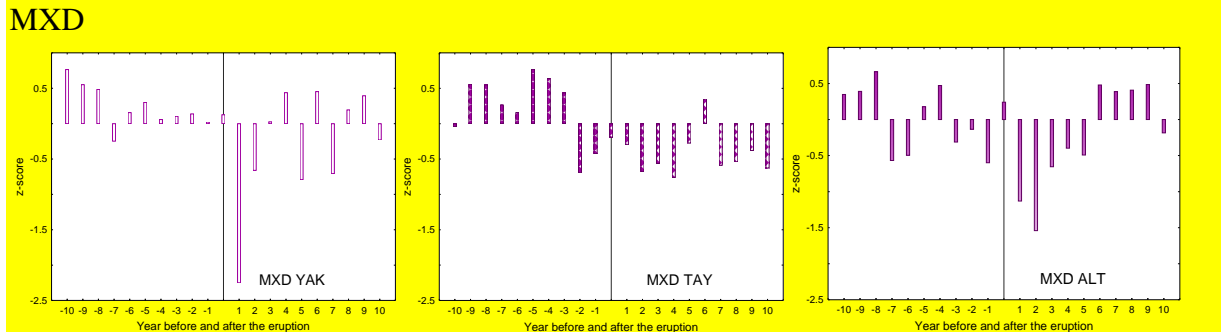
378
379



380
381



382
383



384

385 **Fig. 3.** Superposed epoch analysis of $\delta^{18}\text{O}$, $\delta^{13}\text{C}$, CWT, TRW and MXD chronologies for each
386 study site Yakutia (YAK), Taimyr (TAY) and Altai (ALT), and for the volcanic eruptions in
387 CE 535, 540, 1257, 1641, 1815 and 1991.

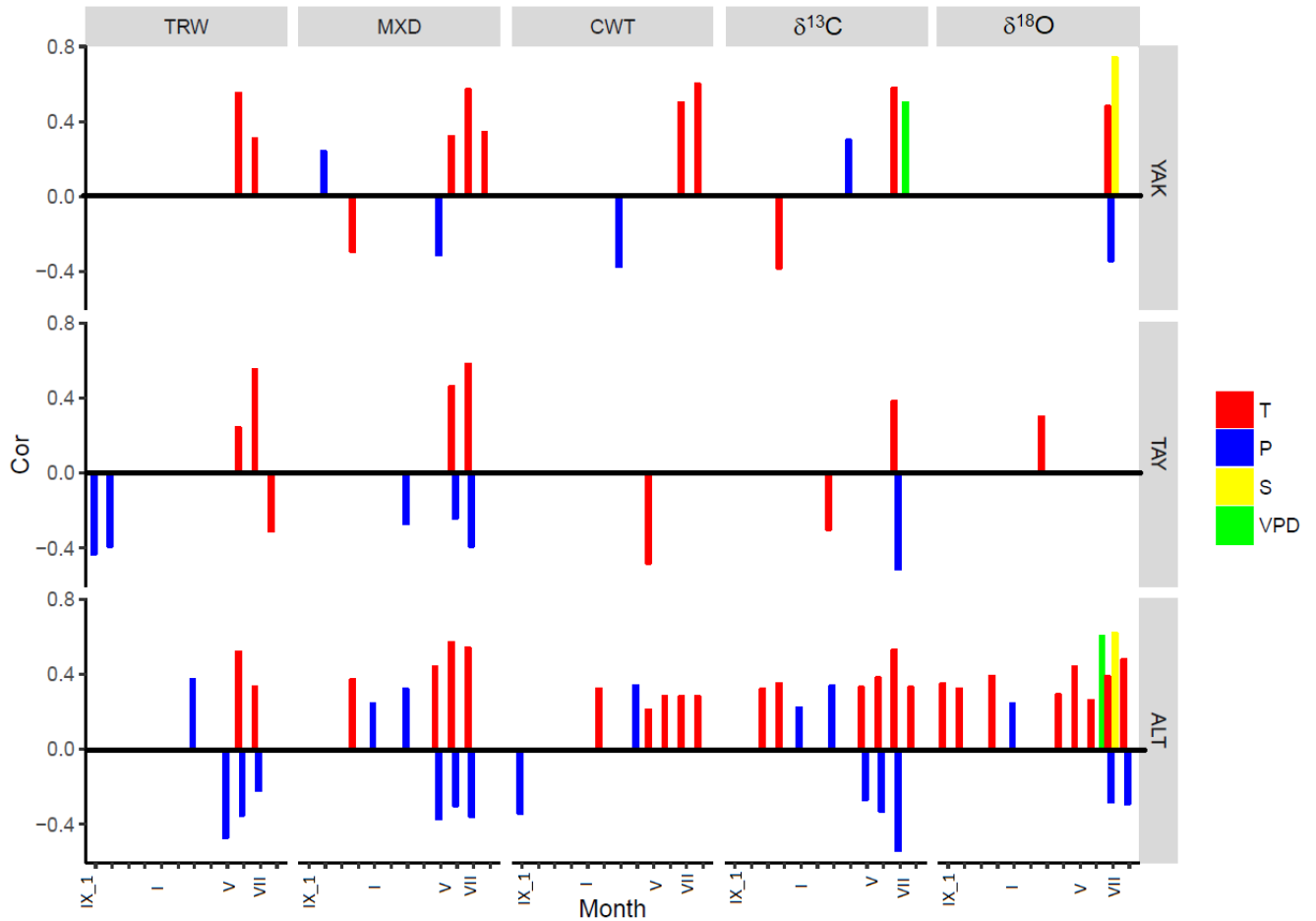
388

389 *3.2. Tree-ring proxies versus meteorological series*

390

391 *3.2.1. Monthly air temperatures and sunshine duration*

392 Bootstrapped functions evidence significant positive correlations ($p < 0.05$) between TRW and
393 MXD chronologies and mean summer (June-July) temperatures at all sites. Temperatures at the
394 beginning (June) and the end of the growing season (mid-August) influenced the MXD chro-
395 nology in ALT ($r = 0.57$) and YAK ($r = 0.55$), respectively (Fig. 4). July temperatures appear
396 as a key factor for determining tree growth as they significantly impact CWT, $\delta^{13}\text{C}$, and $\delta^{18}\text{O}$
397 (with the exception of TAY for the latter) chronologies ($r = 0.28-0.60$) at YAK and ALT.



398
 399 **Fig. 4.** Significant correlation coefficients between tree-ring parameters: TRW, MXD, CWT,
 400 $\delta^{13}C$ and $\delta^{18}O$ versus weather station data: temperature (T, red), precipitation (P, blue), vapor
 401 pressure deficit (VPD, green), and sunshine duration (S, yellow) from September of the previ-
 402 ous year to August of the current year for three study sites were calculated. Table 2 lists stations
 403 used in the analysis.

404
 405 Correlation analysis between July temperature and July sunshine duration showed significant
 406 correlation for YAK ($r=0.56$) and ALT ($r=0.34$). July sunshine duration are strongly and posi-
 407 tively correlated with $\delta^{18}O$ in larch tree-ring cellulose chronologies from YAK ($r=0.73$) and
 408 ALT ($r=0.51$) for the period 1961-2000.

409
 410 *3.2.2. Monthly precipitation*

411 The strongest July precipitation signal is observed at ALT ($r=-0.54$) and TAY ($r=-0.51$) with
412 $\delta^{13}\text{C}$ chronologies ($p<0.05$). In addition, at ALT a positive relationship is observed between
413 March precipitation and TRW ($p<0.05$) ($r=0.37$), MXD ($r=0.32$), while April precipitation with
414 CWT ($r=0.34$), respectively. At YAK, July precipitation showed negative relationship with
415 $\delta^{18}\text{O}$ in tree-ring cellulose ($r=-0.34$; $p<0.05$) only.

416

417 3.2.3. Vapor pressure deficit (VPD)

418 June VPD is significantly and positively correlated with the $\delta^{18}\text{O}$ chronology from ALT ($r=0.67$
419 $p<0.05$, respectively) for the period 1950-2000. The $\delta^{13}\text{C}$ in tree-ring cellulose from YAK cor-
420 relate with July VPD only ($r=0.69$ $p<0.05$). We did not find a significant influence of VPD in
421 TAY tree-ring and stable isotope parameters.

422

423 3.2.4. Synthesis of the climate data analysis

424 In summary, we found that during the instrumental period of weather station observations (Ta-
425 ble 2) mainly summer temperature influenced TRW, MXD and CWT from the high-latitude
426 sites (YAK, TAY), while stable carbon and oxygen isotopes were affected by summer precipi-
427 tation (YAK, TAY, ALT), sunshine duration (YAK, ALT), and vapor pressure deficit (YAK,
428 ALT) signals.

429

430 3.3. Response of Siberian larch trees to climatic changes after the major volcanic eruptions

431 Based on the statistical analysis above for the calibration period, we assumed that these rela-
432 tionships would not change over time and will provide information about climatic changes dur-
433 ing past volcanic periods (Fig. 5).



Fig. 5. Response of larch trees from Siberia to the CE volcanic eruptions (Table 1) with per-
 centile of distribution considered as very extreme (< 5th, intensive color), extreme (>5th, <10th,
 light color) and non-extreme (>10th, white color). July temperature changes presented as a
 square from **heavy blue** (cold) to **light blue** (moderate). Summer vapor pressure deficit (VPD)
 variabilities are shown as a circle from **purple** (low), **light purple** (moderate decrease) to **or-
 ange** (increase, developing to dry air). July precipitation presented as a rhomb from **heavy tur-
 quoise** (wet), **light blue** (moderate) to **orange** (dry). Low July sunshine duration shown as
 black triangle, while high – as yellow.

445

446 *3.3.1. Temperature proxies*

447 We found strong summer air temperature anomalies at all sites after the CE 535 and 1257 vol-
448 canic eruptions. The temperature decrease was found in the TRW and CWT datasets at all sites,
449 and also in the MXD datasets at YAK and ALT (Fig. 5). For the volcanic eruptions in later
450 centuries, the evidence for a decrease in temperature was not as pronounced. Namely, no strong
451 drop in summer temperature was found for ALT in CE 1642 nor 1643, an extreme cold in TAY
452 for 1643 only, while still a cold summer in YAK for both years based on the TRW chronology;
453 1816 was cold only in YAK (based on the CWT chronology), but not at the other sites. CE 1992
454 was recorded as a cold year in MXD and CWT from YAK, but again not for the other sites; CE
455 1993 was an extreme year for ALT based on CWT and $\delta^{18}\text{O}$, while also sunny, which is con-
456 firmed by the local weather station data.

457

458 *3.3.2. Moisture proxies: precipitation and VPD*

459 Based on the climatological analysis with the local weather stations data (Table 2, Fig. 4) for
460 all studied sites we considered $\delta^{13}\text{C}$ in tree-ring cellulose chronologies as proxies for precipita-
461 tion changes. Yet, CWT from ALT could be considered as a proxy with mixed temperature and
462 precipitation signal (Fig. 4, Fig. 5). Therefore, the $\delta^{13}\text{C}$ values, which recorded summer vapor
463 pressure deficit (VPD) showed humid climate conditions for YAK in 536, 541; for TAY in 536,
464 537, 538 and in the year of 541 for ALT. Opposite to other proxies and sites, the year of CE
465 537 in ALT was rather dry (Fig. 5). CE 1258 was dry in TAY, while 1259 - in ALT, opposite
466 to the wet 1258-1259 years in YAK. No anomalies were recorded for the CE 1642 for all studied
467 sites. A rather wet summer was for ALT in CE 1817 compared to 1816 year. CE 1992 in ALT
468 was dry, which corresponds to the weather station data (Fig. 5).

469

470 *3.3.3. Sunshine duration proxies*

471 Instrumental measurements of sunshine duration (Table 2) in YAK and ALT during the recent
472 period showed a significant link with $\delta^{18}\text{O}$ cellulose. Based on this we conclude that sunshine
473 duration decreased significantly in 536 in ALT, while 538, 541, 542, 1258 and 1259 in YAK.
474 Conversely, summer 1993 in ALT was very sunny (Fig. 5).

475

476 **4. Discussion**

477 In this paper, we analyze climatic anomalies in years following selected, large volcanic erup-
478 tions of the CE using long-term, tree-ring multi-proxy chronologies for $\delta^{13}\text{C}$ and $\delta^{18}\text{O}$, TRW,
479 MXD, CWT for the high-latitude (YAK, TAY) and high-altitude (ALT) sites. The main goal
480 was to explore the suitability of the above-mentioned proxies for the detection of abrupt cli-
481 matic changes caused by volcanic eruptions: (i) for each proxy alone, and (ii) for the combined
482 use of all proxies, to reconstruct the respective climatic changes, which should go beyond tem-
483 perature. Since trees as living organisms respond to various climatic impacts, the carbon assim-
484 ilation and growth patterns accordingly leave unique “finger prints” in the photosynthates,
485 which is recorded in the wood of the tree rings specifically and individually for each proxy.

486

487 *4.1. Evaluation of the applied proxies in Siberian tree-ring data*

488 This study clearly shows that each proxy has to be analyzed and interpreted specifically for its
489 validity on each studied site and evaluated for its suitability for the reconstruction of abrupt
490 climatic changes.

491 TRW in temperature-limited environments is a proxy for summer temperature reconstructions,
492 as growth is a temperature-controlled process. Temperature clearly determines the duration of
493 the growing season and the rate of cell division (Cuny et al., 2014). Accordingly, low growing
494 season temperatures are reflected in narrow tree rings. The upper temperature limit is species

495 and biome specific. In most cases tree growth is limited by drought rather than by high temper-
496 atures, since water shortage and VPD increase with increasing temperature. Still this does not
497 make TRW a suitable proxy to determine the influence of water availability and air humidity,
498 especially at the temperature-limited sites.

499 MXD chronologies obtained for the Eurasian subarctic record mainly a July-August tempera-
500 ture signal (Vaganov et al., 1999; Sidorova et al., 2010; Büntgen et al., 2016) and add valuable
501 information about climate conditions toward the end of the growth season. Similarly, CWT is
502 an anatomical parameter, which contains information on carbon sink limitation of the cambium
503 due to extreme cold conditions (Panyushkina et al., 2003; Fonti et al., 2013; Bryukhanova et
504 al., 2015). The clear signal about reduced number of cells within a season, for example, strong
505 decreasing CWT in CE 536 at YAK or formation of frost rings in ALT (CE 536-538, 1259) has
506 been shown in our study.

507 Low $\delta^{13}\text{C}$ values can be explained by a reduction in photosynthesis caused by volcanic dust
508 veils. For the distinction whether $\delta^{13}\text{C}$ is predominantly determined by A_N or g_l the combined
509 evaluation with $\delta^{18}\text{O}$ or TRW is needed. High $\delta^{18}\text{O}$ values indicate high VPD, which induces a
510 reduction in stomatal conductance, reducing the back diffusion of depleted water molecules
511 from the ambient air. This confirms a sunny year **CE 1993** in ALT with warm and dry weather
512 conditions. Interestingly, we also find less negative values for $\delta^{13}\text{C}$ in the same period. This
513 shows that the two isotopes correlate with each other and this indicates the need for a combined
514 evaluation of the C and O isotopes (Scheidegger et al., 2000) taking into account precautions
515 as suggested by Roden and Siegwolf (2012).

516

517 *4.2. Lag between volcanic events and response in tree rings*

518 In most of the discussed events, we observe a certain delay – or lag – between the eruption and
519 the response in tree rings of one year or more (Fig. 3). This lag is explained by the tree's use of

520 stored carbohydrates, which are the substrate for needle and early wood production. These
521 stored carbohydrates carry the isotopic signal of previous years and depending on their remo-
522 bilization and use mask the signals in freshly produced biomass. The delayed signal could also
523 reflect the time needed for the dust veil to be transported to the study sites.

524

525 *4.3. Temperature and sunshine duration changes after stratospheric volcanic eruptions*

526 Correlation functions show that MXD and CWT (with the exception of TAY in the latter case),
527 and to a lesser extent also TRW chronologies, portray the strongest signals for summer (June-
528 August) temperatures. In addition, significant information about sunshine duration can be de-
529 rived from the YAK and ALT $\delta^{18}\text{O}$ series. Thus, we hypothesize that extremely narrow TRW
530 and very negative anomalies observed in the MXD and CWT chronologies of YAK and to a
531 lesser extent at ALT, in CE 536 and 1258 along with low $\delta^{18}\text{O}$ values (except for ALT in CE
532 1257) reflect cold conditions in summer. Presumably, the temperatures were below the thresh-
533 old values for growth (Körner, 2015). This hypothesis of a generalized regional cooling after
534 both eruptions is further confirmed by the occurrence of frost rings at **ALT site** in CE 538, 1259
535 (Myglan et al., 2008; Guillet et al., 2017), as well as in neighboring Mongolia (D'Arrigo et al.,
536 2001). The unusual cooling in CE 536 is also evidenced by a very small number of cells formed
537 at YAK (Churakova (Sidorova) et al., 2014). Although $\delta^{18}\text{O}$ is an indirect proxy for needle
538 temperature, low $\delta^{18}\text{O}$ values in CE 536 and 1258 for YAK and ALT are a result of low irradi-
539 ation, leading to low temperature and low VPD (high stomatal conductance), both likely a result
540 from volcanic dust veils.

541 Similarly, in the aftermath of the Samalas eruption, the persistence of summer cooling is limited
542 to CE 1259 only at the three study sites, which is in line with findings of Guillet et al., (2017).
543 Interestingly, a slight decrease in oxygen isotope chronologies – which can be related to low

544 levels of summer sunshine duration (i.e. low leaf temperatures) – allows for hypothesizing that
545 cool conditions could have prevailed.

546 For all later high-magnitude CE eruptions, temperature-sensitive tree-ring proxies do not evi-
547 dence a generalized drop in summer temperatures. Paradoxically, the impacts of the Tambora
548 eruption, known for its triggering of a widespread “year without summer” (Harrington, 1992),
549 did only induce abnormal MXD at YAK, but no anomalies are observed at sites TAY and ALT,
550 except for the positive deviation of $\delta^{13}\text{C}$ in TAY and negative anomaly in CE 1817 for ALT
551 (Fig. 2). While these findings may seem surprising, they are in line with the TRW and MXD
552 reconstructions of Briffa et al., (1998) or Guillet et al., (2017), who found limited impacts of
553 the CE 1815 Tambora event in Eastern Siberia and Alaska using TRW and MXD data only.
554 The inclusion of CWT chronologies, not used in their reconstructions, further confirm the ab-
555 sence of a significant cooling in this region following the second largest eruption of the last
556 millennium.

557 Finally, in CE 1992, our results evidence cold conditions in YAK, which is consistent with
558 weather observations showing that the below-average anomalies in summer temperatures (after
559 Pinatubo eruption) were indeed limited to Northeastern Siberia (Robock, 2000). As both iso-
560 topes indicate a reduction in stomatal conductance, we found that warm (in agreement with
561 MXD and CWT) and dry conditions were prevalent for ALT at this time. This isotopic constel-
562 lation was confirmed by the positive relationships between VPD and $\delta^{18}\text{O}$ and $\delta^{13}\text{C}$ for ALT.

563 However, temperature and sunshine duration are not always highly coherent over time due to
564 the influence of other factors, like Arctic Oscillations as it was suggested for Fennoscandia
565 regions by Loader et al. (2013).

566

567 *4.4. Moisture changes*

568 Water availability is a key parameter for Siberian trees as they are growing under extremely
569 continental conditions with hot summers and cold winters, and even more so with very low
570 annual precipitation (Table 2). Continuous permafrost, in addition, is playing a crucial role, and
571 can be considered as a buffer for additional water sources during hot summers (Sugimoto et al.,
572 2002; Boike et al., 2013; Saurer et al., 2016). Yet, thawed permafrost water is not always avail-
573 able for roots due to the surficial structure of the root plate or extremely cold water temperature
574 (close to 0°C), which can hardly be utilized by trees (Churakova (Sidorova) et al., 2016). Thus,
575 Siberian trees are highly susceptible to drought, induced by dry and warm air during July and
576 therefore the stable carbon isotopes can be sensitive indicators of such conditions. After vol-
577 canic eruptions, however, low light intensity due to dust veils induce low temperatures and
578 reduced VPD, the driver for evapotranspiration. Under such conditions drought stress is un-
579 likely to occur. However, the transition phases with changes from cool and moist to warm and
580 dry conditions are more critical when drought is more likely to occur.

581 In our study, higher $\delta^{13}\text{C}$ values in tree-ring cellulose indicate increasing drought conditions as
582 a consequence of reduced precipitation for two years after the CE 1257 volcanic eruption at all
583 three sites. No further extreme hydro-climatic anomalies occurred at Siberian sites in the after-
584 math of the Pinatubo eruption.

585

586 *4.5. Synthesized interpretation from the multi-parameter tree-ring proxies*

587 Our analysis demonstrates the added value of a tree-ring derived multi-proxy approach to better
588 capture the climatic variability after large volcanic eruptions. Besides the well-documented ef-
589 fects of temperature derived from TRW and MXD, CWT, stable carbon and oxygen isotopes
590 in tree-ring cellulose provide important and complementary information about moisture and
591 sunshine duration changes (an indirect proxy for leaf temperature effective for air-to-leaf VPD)
592 after stratospheric volcanic eruptions.

593 In detail, our results reveal a complex behavior of the Siberian climatic system to the strato-
594 spheric volcanic eruptions of the Common Era. The CE 535 and CE 1257 Samalas eruptions
595 caused substantial cooling – very likely induced by dust veils (Churakova (Sidorova) et al.,
596 2014; Guillet et al., 2017; Helama et al., 2018) – as well as humid conditions at the high-latitude
597 sites. Conversely, only local climate responses were observed after the CE 1641 Parker, 1815
598 Tambora, and 1991 Pinatubo eruptions. Similar site-dependent impacts were found in CE 1453,
599 1458 and 1601 (Fig. S1), frequently referred to as the coldest summers of the last millennium
600 in the Northern Hemisphere based on TRW and MXD reconstructions (Schneider et al., 2015;
601 Stoffel et al., 2015; Wilson et al., 2016; Guillet et al., 2017). This absence of widespread and
602 intense cooling or reduction of precipitation over vast regions of Siberia may result from the
603 location and strength of the volcanic eruption, atmospheric transmissivity as well as from the
604 modulation of radiative forcing effects by regional climate variability. These results are con-
605 sistent with other regional studies, which interpreted the spatio-temporal heterogeneity of tree
606 responses to past volcanic events (Wiles et al., 2014; Esper et al., 2017; Barinov et al., 2018) in
607 terms of regional climate peculiarities.

608

609 5. Conclusions

610 In this study, we demonstrate that the consequences of volcanic eruptions on climate are ra-
611 ther complex between sites and among events. Our study highlighted a common difficulty of
612 climate reconstructions from various tree-ring proxies, where often not all frequencies,
613 seasonal length can be reconstructed with the same confidence. The differences between
614 proxies could be explained by the combined influence of different climate parameters, which
615 is specifically difficult to separate for temperature-limited environment, different seasonality
616 and different response patterns to temperature and precipitation changes in the permafrost
617 zone.

618 That said, we also show that each proxy alone cannot provide the full information on an erup-
619 tion but that it contributes to the understanding and the full picture by adding to a single, spe-
620 cific factor, which is critical for a comprehensive description of climate dynamics induced by
621 volcanism and the inclusion of these phenomena in global climate models.

622 Therefore, the application of a multiple tree-ring parameter approach provides detailed infor-
623 mation. **Analyses of large number of samples and intensive investigations of Siberian sites for**
624 **the comparative analysis is urgently needed. Because, it become obvious that** the multi-proxy
625 approach allows refining the interpretation and improves our understanding of the heterogene-
626 ity of climatic signals after CE stratospheric volcanic eruptions, which are recorded in multiple
627 tree-ring and stable isotope parameters from the vast Siberian regions.

628

629 **Author contribution:** TRW analysis was performed at V.N. Sukachev Institute of Forest SB
630 RAS by O.V. Churakova (Sidorova), D.V. Ovchinnikov, V.S. Myglan and O.V. Naumova.
631 CWT analysis was carried out at the V. N. Sukachev Institute of Forest SB RAS, Krasnoyarsk,
632 Russia by M. Fonti and at the University of Arizona by I. Panyushkina. Stable isotope analysis
633 was conducted at the Paul Scherrer Institute (PSI), by O. V. Churakova (Sidorova), M. Saurer,
634 and R. Siegwolf. MXD measurements were realized with a DENDRO Walesh 2003 densitom-
635 eter at WSL and at the V.N. Sukachev Institute of Forest SB RAS, Krasnoyarsk, Russia by O.
636 V. Churakova (Sidorova) and A. V. Kirilyanov. Samples from YAK and TAY were collected
637 by M. M. Naurzbaev. All authors contributed significantly to the data analysis and paper writ-
638 ing.

639 **Acknowledgements:** This work was supported by Marie Curie International Incoming Fellow-
640 ship [EU_ISOTREC 235122], Re-Integration Marie Curie Fellowship [909122] and UFZ
641 scholarship [2006], RFBR [09-05-98015_r_sibir_a] granted to Olga V. Churakova (Sidorova);
642 SNSF M. Saurer [200021_121838/1]; Era.Net RUSPlus project granted to M. Stoffel [SNF

643 IZRPZO_164735] and RFBR [№ 16-55-76012 Era_a] granted to E.A. Vaganov; project granted
644 to Vladimir S. Myglan RNF, Russian Scientific Fond [№ 15-14-30011]; Alexander V. Kirdy-
645 nov was supported by the Ministry of Education and Science of the Russian Federation
646 [#5.3508.2017/4.6] and RSF [#14-14-00295]; Scientific School [3297.2014.4] granted to Eu-
647 gene A. Vaganov; and US National Science Foundation (NSF) grants [#9413327, #970966,
648 #0308525] to Malcolm K. Hughes and US CRDF grant # RC1-279, to Malcolm K. Hughes
649 and Eugene A. Vaganov. We thank Tatjana Boettger for her support and access to the stable
650 isotope facilities within UFZ Haale/Saale scholarship 2006; Anne Verstege, Daniel Nievergelt
651 for their help with sample preparation for the MXD and Paolo Cherubini for providing lab
652 access at the Swiss Federal Institute for Forest, Snow and Landscape Research (WSL).
653 We thank two anonymous reviewers for their constructive comments on this manuscript.

654 **Figure legend**

655

656 **Fig. 1.** Map with the locations of the study sites (stars) and volcanic eruptions (black dots)
657 considered in this study (a). Annual tree-ring width index (light lines) and smoothed by 51-year
658 Hamming window (bold lines) chronologies from northeastern Yakutia (YAK - **blue**, b)
659 (Hughes *et al.*, 1999; Sidorova 2003), eastern Taimyr (TAY - **green**, c) (Naurzbaev *et al.*,
660 2002), and Russian Altai (ALT - **red**, d) (Myglan *et al.*, 2009) were constructed based on larch
661 trees (Photos: V. Myglan – ALT, M. M. Naurzbaev – YAK, TAY).

662

663 **Fig. 2.** Normalized (z-score) individual tree-ring index chronologies (TRWi, **black**), maximum
664 latewood density (MXD, **purple**), cell wall thickness (CWT, **green**), $\delta^{13}\text{C}$ (**red**) and $\delta^{18}\text{O}$ (**blue**)
665 in tree-ring cellulose chronologies from YAK, TAY and ALT for the specific periods 10 years
666 before and after the eruptions CE 535, 1257, 1640, 1815 and 1991 are presented. Vertical lines
667 showed year of the eruptions.

668

669 **Fig. 3.** Superposed Epoch Analysis (SEA) of $\delta^{18}\text{O}$, $\delta^{13}\text{C}$, CWT, TRW and MXD chronologies
670 for each study site by combination of the major volcanic eruptions CE 535, 1257, 1641, 1815
671 and 1991.

672

673 **Fig. 4.** Significant correlation coefficients between tree-ring parameters and weather station
674 data: temperature (**red**), precipitation (**blue**), vapor pressure deficit (**green**), and sunshine du-
675 ration (yellow) from September of the previous year to August of the current year for three
676 study sites were calculated. Table 2 lists stations used in the analysis.

677

678 **Fig. 5.** Response of larch trees from Siberia to the CE volcanic eruptions (Table 1) with per-
679 centile of distribution considered as very extreme (< 5th, intensive color), extreme (>5th, <10th,
680 light color) and non-extreme (>10th, white color). July temperature changes presented as a
681 square from **heavy blue** (cold) to **light blue** (moderate). Summer vapor pressure deficit (VPD)
682 variabilities are shown as a circle from **purple** (low), **light purple** (moderate decrease) to **or-**
683 **ange** (increase, developing to dry air). July precipitation presented as a rhomb from **heavy tur-**
684 **quoise** (wet), **light blue** (moderate) to **orange** (dry). Low July sunshine duration shown as
685 black triangle, while high – as yellow.

686

687 **Table 1.** List of stratospheric volcanic eruptions used in the study.

688

689 **Table 2.** Summary of tree-ring sites in northeastern Yakutia (YAK), eastern Taimyr (TAY) and
690 Altai (ALT), and weather stations used in the study. Monthly air temperature (T, °C), precipi-
691 tation (P, mm), sunshine duration (S, h/month) and vapor pressure deficit (VPD, kPa) data were
692 used from available meteorological database <http://aisori.meteo.ru/ClimateR>.

693

694

695 **References**

- 696 Abaimov, A.P., Bondarev, A.I., Yzranova, O.V., Shitova, S.A.: Polar forests of Krasnoyarsk
697 region. Nauka Press, Novosibirsk. 208 p., 1997.
- 698 Battipaglia, G., Cherubini, P., Saurer, M., Siegwolf, R.T.W., Strumia, S., Cotrufo, M.F.: Vol-
699 canic explosive eruptions of the Vesuvio decrease tree-ring growth but not photosyn-
700 thetic rates in the surrounding forests. *Global Change Biology*. 13, 1-16, 2007.
- 701 Barinov, V.V., Myglan, V.S., Taynik, A.V., Ojdupaa, O.Ch., Agatova, A.R., Churakova (Si-
702 dorova) O.V. Extreme climatic events in Altai-Sayan region as indicator of major
703 volcanic eruptions. *Geophysical processes and biosphere*. 17, 45-61, 2018. doi:
704 10.21455/GPB2018.3-3.
- 705 Beerling, D.J., Woodward, F.I.: Ecophysiological responses of plants to global environmental
706 change since the last glacial maximum. *New Phytologist*. 125, 641–648, 1994.
- 707 Boettger T., Haupt, M., Knöller, K., Weise, S., Waterhouse, G.S. ... Schleser, G.H.: Wood
708 cellulose preparation methods and mass spectrometric analyses of $\delta^{13}\text{C}$, $\delta^{18}\text{O}$, and non
709 ex-changeable $\delta^2\text{H}$ values in cellulose, sugar, and starch: An inter-laboratory compar-
710 ison, *Anal. Chem.* 79, 4603–4612, doi:10.1021/ac0700023, 2007.
- 711 Boike, J., Kattenstroth, B., Abramova, K., Bornemann, N., Cherverova, A., Fedorova, I., Fröb,
712 K., Grigoriev, M., Grüber, M., Kutzbach, L., Langer, M., Minke, M., Muster, S., Piel,
713 K., Pfeiffer, E.-M., Stoff, G., Westermann, S., Wischnewski, K., Wille, C., Hubberten,
714 H.-W.: Baseline characteristics of climate, permafrost and land cover from a new per-
715 mafrost observatory in the Lena Rive Delta, Siberia (1998-2011). *Biogeosciences*. 10,
716 2105-2128, 2013.
- 717 Briffa, K.R., Jones, P.D., Schweingruber, F.H., Osborn, T.J.: Influence of volcanic eruptions
718 on Northern Hemisphere summer temperature over the past 600 years. *Nature*. 393,
719 450–455, 1998.

- 720 Bryukhanova, M.V., Fonti, P., Kirilyanov, A.V., Siegwolf, R., Saurer, M., Pochebyt, N.P., Chu-
721 rakova (Sidorova), O.V., Prokushkin, A.S.: The response of $\delta^{13}\text{C}$, $\delta^{18}\text{O}$ and cell anat-
722 omy of *Larix gmelinii* tree rings to differing soil active layer depths. *Dendrochronolo-*
723 *gia*. 34, 51-59, 2015.
- 724 Büntgen, U., Myglan, V.S., Ljungqvist, F.C., McCormick, M., Di Cosmo, N., Sigl M., ...Kir-
725 dyanov, A.V.: Cooling and societal change during the Late Antique Little Ice Age
726 from 536 to around 660 AD. *Nature Geoscience*. 9, 231-236, 2016.
- 727 Cernusak, L., Ubierna, N., Winter, K., Holtum, J.A.M., Marshall, J.D., Farquhar, G.D.: Envi-
728 ronmental and physiological determinants of carbon isotope discrimination in terres-
729 trial Plants. *Transley Review New Phytologist*. 200, 950-965, 2013.
- 730 Cernusak, L., Barbour, M., Arndt, S., Cheesman, A., English, N., Field, T., Helliker, B., Hol-
731 loway-Phillips, M., Holtum, J., Kahmen, A., Mcnerney F, Munksgaard N, Simonin K,
732 Song X, Stuart-Williams H, West J and Farquhar G.: Stable isotopes in leaf water of
733 terrestrial plants. *Plant, Cell & Environment*. 39 (5), 1087-1102, 2016.
- 734 Churakova (Sidorova), O.V., Bryukhanova, M., Saurer, M., Boettger, T., Naurzbaev, M.,
735 Myglan, V.S., Vaganov, E.A., Hughes, M.K., Siegwolf, R.T.W.: A cluster of strato-
736 spheric volcanic eruptions in the AD 530s recorded in Siberian tree rings. *Global and*
737 *Planetary Change*. 122, 140-150., 2014.
- 738 Churakova (Sidorova), O.V., Shashkin, A.V., Siegwolf, R., Spahni, R., Launois, T., Saurer M.,
739 Bryukhanova, M.V., Benkova, A.V., Kupzova, A.V., Vaganov, E.A., Peylin, P., Mas-
740 son-Delmotte, V., Roden, J.: Application of eco-physiological models to the climatic
741 interpretation of $\delta^{13}\text{C}$ and $\delta^{18}\text{O}$ measured in Siberian larch tree-rings. *Dendro-*
742 *chronologia*, doi:10.1016/j.dendro.2015.12.008, 2016.

- 743 Cook, E., Briffa, K., Shiyatov, S., Mazepa, V.: Tree-ring standardization and growth trend es-
744 timation. In: *Methods of dendrochronology: applications in the environmental sci-*
745 *ences*, Eds: Cook, E.R., Kairiukstis, L.A. 104-123, 1990.
- 746 Cook, E.R., Krusic, P.J.: A Tree-Ring Standardization Program Based on Detrending and Au-
747 toregressive Time Series Modeling, with Interactive Graphics (ARSTAN). (Ed. by
748 E.R., Cook and P.J., Krusic), 2008.
- 749 Craig, H.: Isotopic variations in meteoric waters. *Science*. 133, 1702– 1703, 1961.
- 750 Crowley, T.J., Unterman, M.B.: Technical details concerning development of a 1200 yr.
751 proxy index for global volcanism. *Earth Syst. Sci. Data*. 5, 187-197, 2013.
- 752 Cuny, H.E., Rathgeber, C.B.K., Frank, D., Fonti, P., Fournier, M.: Kinetics of tracheid devel-
753 opment explain conifer tree-ring structure. *New Phytologist*, 203, 1231–1241, 2014.
- 754 D'Arrigo, R.D., Jacoby, G.C., Frank, D., Pederson, N.D., Cook, E., Buckley, B.M., Nachin, B.,
755 Mijidorj, R., Dugarjav, C.: 1738-years of Mongolian temperature variability inferred
756 from a tree-ring width chronology of Siberian pine. *Geophysical Research Letters*.
757 Vol. 28 (3), 543-546, 2001.
- 758 Dansgaard, W.: Stable isotopes in precipitation. *Tellus*. 16, 436–468, 1964.
- 759 Dawson, T.E., Mambelli, S., Plamboeck, A.H., Templer, P.H., Tu, K.P.: Stable isotopes in plant
760 ecology *Ann. Review of Ecology and Systematics*. 33, 507-559, 2004.
- 761 Dongmann, G., Förstel, H., Wagener, K.: ^{18}O -rich oxygen from land photosynthesis. *Nature*
762 *New Biol*. 240, 127–128, 1972.
- 763 Eschbach, W., Nogler, P., Schär, E., Schweingruber, F.H.: Technical advances in the radioden-
764 sitometrical determination of wood density. *Dendrochronologia*. 13, 155–168, 2015.
- 765 Esper, J., Büntgen, U., Hartl-Meier, C., Oppenheimer, C., Schneider, L.: Northern Hemisphere
766 temperature anomalies during 1450s period of ambiguous volcanic forcing. *Bull. Vol-*
767 *canology*. 79, 41, 2017.

- 768 Farquhar, G. D.: Eds. *Stable Isotopes and Plant Carbon-Water Relations*. Academic Press, San
769 Diego. 47–70, 1982.
- 770 Farquhar, G.D., Ehleringer, J.R., Hubick, K.T.: *Annu. Rev. Plant Physiol. Plant Mol. Biol.* 40,
771 503 p, 1989.
- 772 Farquhar, G.D., Lloyd, J.: Carbon and oxygen isotope effects in the exchange of carbon dioxide
773 between terrestrial plants and the atmosphere. In: Ehleringer, J.R., Hall, A.E., Far-
774 quhar, G.D. (Eds) *Stable Isotopes and Plant Carbon-Water Relations*. Academic Press,
775 San Diego, 47–70, 1993.
- 776 Fonti, P., Bryukhanova, M.V., Myglan, V.S., Kirilyanov, A.V., Naumova, O.V., Vaganov,
777 E.A.: Temperature-induced responses of xylem structure of *Larix sibirica* (Pinaceae)
778 from Russian Altay. *American Journal of Botany*. 100 (7), 1-12, 2013.
- 779 Francey, R.J., Allison, C.E., Etheridge D.M., Trudinger, C.M., Langenfelds, R.L., Michel, E.,
780 Steele, L.P.: A 1000-year high precision record of $\delta^{13}\text{C}$ in atmospheric CO_2 . *Tellus*.
781 Ser. B (51), 170-193, 1999.
- 782 Fritts, H.C.: *Tree-rings and climate*. London. New York; San Francisco: Acad. Press. 567 p,
783 1976.
- 784 Furst, G.G.: *Methods of Anatomical and Histochemical Research of Plant Tissue*. Nauka, Mos-
785 cow. 156 p, 1979.
- 786 Gao, C., Robock, A., Ammann, C.: Volcanic forcing of climate over the past 1500 years: An
787 improved ice core-based index for climate models. *J. Geophys. Res. Atmos.*
788 113:D23111. doi:10.1029/2008jd010239, 2008.
- 789 Gennaretti, F., Huard, D., Naulier, M., Savard, M., Bégin, C., Arseneault, D., Guiot, J.: Bayes-
790 ian multiproxy temperature reconstruction with black spruce ring widths and stable
791 isotopes from the northern Quebec taiga. *Clim. Dyn.* doi: 10.1007/s00382-017-3565-
792 5, 2017.

- 793 Gillett, N.P., Weaver, A.J., Zwiers, F.W. Wehner, M.F.: Detection of volcanic influence on
794 global precipitation. *Geophysical Research Letters*, 31 (12),
795 doi:10.1029/2004GL020044 R, 2004.
- 796 Groisman, P.Ya.: Possible regional climate consequences of the Pinatubo eruption. *Geophys.*
797 *Res. Lett.*, 19, 1603–1606, 1992.
- 798 Gu, L., Baldocchi, D.D., Wofsy, S.C., Munger, J.W., Michalsky, J.J., Urbanski, S.P., Boden,
799 T.A.: Response of a deciduous forest to the Mount Pinatubo eruption: Enhanced photo-
800 tosynthesis, *Science*. 299 (5615), 2035–2038, 2003.
- 801 Guillet, S., Corona, C., Stoffel, M., Khodri M., Lavigne F., Ortega, P.,....Oppenheimer, C.:
802 Climate response to the 1257 Samalas eruption revealed by proxy records. *Nature ge-*
803 *oscience*, doi:10.1038/ngeo2875, 2017.
- 804 Hansen, J., Sato, M., Ruedy, R., Lacis, A., Asamoah, K., Borenstein S.,Wilson, H.: A
805 Pinatubo climate modeling investigation. In *The Mount Pinatubo Eruption: Effects on*
806 *the Atmosphere and Climate*, NATO ASI Series Vol. I 42. G. Fiocco, D. Fua, and G.
807 Visconti, Eds. Springer-Verlag, 233-272, 1996.
- 808 Harrington, C.R.: *The Year without a summer? World climate in 1816*. Ottawa: Canadian
809 Museum of Nature, ISBN 0660130637, 1992.
- 810 Helama, S., Arppe, L., Uusitalo, J., Holopainen, J., Mäkelä, H.M., Mäkinen, H., Mielikäinen,
811 K., Nöjd, P., Sutinen, R., Taavitsainen, J.-P., Timonen, M., Oinonen, M.: Volcanic
812 dust veils from sixth century tree-ring isotopes linked to reduced irradiance, primary
813 production and human health. *Scientific reports* 8, 1339. doi:10.1038/s41598-018-
814 19760-w, 2018.
- 815 Hughes, M.K., Vaganov, E.A., Shiyatov, S.G., Touchan, R. & Funkhouser, G.: Twentieth-
816 century summer warmth in northern Yakutia in a 600-year context. *The Holocene*.
817 9(5), 603-608, 1999.

- 818 Iles, C.E., Hegerl, G.C.: The global precipitation response to volcanic eruptions in the CMIP5
819 models. *Environ. Res. Lett.* 9, doi:10.1088/1748-9326/9/10/104012, 2014.
- 820 Joseph, R., Zeng, N.: Seasonally modulated tropical drought induced by volcanic aerosol. *J.*
821 *Climate*, 24, 2045–2060, 2011.
- 822 Körner, Ch.: Paradigm shift in plant growth control. *Curr. Opinion Plant Biol.* 25, 107-114,
823 2015.
- 824 Lavigne, F., Degeai, J.-P., Komorowski, J.-C., Guillet, S., Robert, V., Lahitte, P., Oppenhei-
825 mer, C., Stoffel, M., Vidal, C.M., Suro, I.P., Wassmer, P., Hajdas, I., Hadmoko, D.S.,
826 Belizal, E.: Source of the great A.D. 1257 mystery eruption unveiled, Samalas vol-
827 cano, Rinjani Volcanic Complex, Indonesia. *Proc Natl Acad Sci* 110, 16742–16747,
828 doi:10.1073/pnas.1307520110, 2013.
- 829 Lehmann, M.M., Goldsmith, G.T., Schmid, L., Gessler, A., Saurer, M., Siegwolf, R.T.W.: The
830 effect of ¹⁸O-labelled water vapour on the oxygen isotope ratio of water and assimilates
831 in plants at high humidity. *New Phytologist*. 217, 1, 105-116. doi: 10.1111/nph.14788,
832 2018.
- 833 Lenz, O., Schär, E., Schweingruber F.H.: Methodische Probleme bei der radiographisch-densi-
834 tometrischen Bestimmung der Dichte und der Jahrrinbreiten von Holz. *Holzforschung*,
835 30, 114-123, 1976.
- 836 Loader, N.J., Robertson, I., Barker, A.C., Switsur, V.R., Waterhouse, J.S.: Improved technique
837 for the batch processing of small whole wood samples to alpha-cellulose. *Chemical*
838 *Geology*. 136, 313-317, 1997.
- 839 Loader, N.J., Young, G.H.F., Grudd, H., McCarroll.: Stable carbon isotopes from Torneträsk,
840 norther Sweden provide a millennial length reconstruction of summer sunshine and its
841 relationship to Arctic circulation. *Quaternary Science Reviews*. 62, 97-113, 2013.

- 842 McCarroll, D., Loader, N.J.: Stable isotopes in tree rings. *Quaternary Science Review*. 23, 771-
843 801, 2004.
- 844 Meronen, H., Henriksson, S.V., Räisänen, P., Laaksonen, A.: Climate effects of northern hem-
845 isphere volcanic eruptions in an Earth System Model. *Atmospheric Research*, 114-
846 115: 107-118, 2012.
- 847 Munro, M.A.R., Brown, P.M., Hughes, M.K., Garcia, E.M.R.: Image analysis of tracheid
848 dimensions for dendrochronological use. *Radiocarbon*, Eds. by M.D. Dean, J.
849 Swetnam T), pp. 843-851. Tucson, Arizona, 1996.
- 850 Myglan, V.S., Oidupaa, O. Ch., Kirilyanov, A.V., Vaganov, E.A.: 1929-year tree-ring chronol-
851 ogy for Altai-Sayan region (Western Tuva). *Journal of archeology, ethnography and*
852 *anthropology of Eurasia*. 4 (36), 25-31, 2008.
- 853 Naurzbaev, M.M., Vaganov, E.A., Sidorova, O.V., Schweingruber, F.H.: Summer temperatures
854 in eastern Taimyr inferred from a 2427-year late-Holocene tree-ring chronology and
855 earlier floating series. *The Holocene*. 12(6), 727-736, 2002.
- 856 Panofsky, H.A., Brier, G.W.: *Some applications of statistics to meteorology*. University Park,
857 PA. Mineral industries extension services, college of mineral industries, Pennsylvania
858 State University, 1958.
- 859 Panyushkina, I.P., Hughes, M.K., Vaganov, E.A., Munro, M.A.R.: Summer temperature in
860 northern Yakutia since AD 1642 reconstructed from radial dimensions of larch trache-
861 ids. *Canadian Journal of Forest Research*. 33, 1-10, 2003.
- 862 Peng, Y., Shen, C., Wang, W.-C., Xu, Y.: Response of summer precipitation over Eastern China
863 to large volcanic eruptions. *Journal of Climate*. 23, 818-824, 2009.
- 864 R Core Team.: *R: A Language and Environment for Statistical Computing*. Vienna, Austria,
865 2016.
- 866 Robock, A.: Volcanic eruptions and climate. *Reviews of Geophysics*. 38(2), 191-219, 2000.

- 867 Robock, A., Liu, Y.: The volcanic signal in Goddard Institute for Space Studies three-dimensional model simulations. *J. Climate*. 7, 44-55, 1994.
- 868
- 869 Roden, J.S., Siegwolf, R.: Is the dual isotope conceptual model fully operational? *Tree Physiology*. 32, 1179-1182, 2012.
- 870
- 871 Saurer, M., Kirilyanov, A.V., Prokushkin, A.S., Rinne K.T., Siegwolf, R.T.W.: The impact of an inverse climate–isotope relationship in soil water on the oxygen-isotope composition of *Larix gmelinii* in Siberia. *New Phytologist*. 109, 3, 955-964, 2016.
- 872
- 873
- 874 Saurer, M., Robertson, I., Siegwolf, R., Leuenberger, M.: Oxygen isotope analysis of cellulose: an interlaboratory comparison. *Analytical chemistry*, 70, 2074-2080, 1998.
- 875
- 876 Saurer, M., Kirilyanov, A. V., Prokushkin, A. S., Rinne, K. T., Siegwolf, R.T.W.: The impact of an inverse climate-isotope relationship in soil water on the oxygen-isotope composition of *Larix gmelinii* in Siberia. *New Phytologist*. 209(3), 955-964, 2016.
- 877
- 878
- 879 Scheidegger, Y., Saurer, M., Bahn, M., Siegwolf, R.: Linking stable oxygen and carbon isotopes with stomatal conductance and photosynthetic capacity: a conceptual model. *Oecologia*. 125, 350–357. DOI: 10.1007/s004420000466, 2000.
- 880
- 881
- 882 Schneider, L., Smerdon, J.E., Büntgen, U., Wilson, R.J.S., Myglan, V.S., Kirilyanov, A.V., Esper, J.: Revising mid-latitude summer temperatures back to A.D. 600 based on a wood density network. *Geophys. Res. Lett.* 42, GL063956, Doi:10.1002/2015gl063956, 2015.
- 883
- 884
- 885
- 886 Schweingruber, F.H.: *Tree rings and environment dendroecology*. Paul Haupt Publ Bern, Stuttgart, Vienna 1996. pp. 609, 1996.
- 887
- 888 Sidorova, O.V., Naurzbaev, M.M.: Response of *Larix cajanderi* to climatic changes at the upper timberline and in the Indigirka River valley. *Lesovedenie (in Russian)*. 2, 73-75, 2002.
- 889

- 890 Sidorova, O.V.: Long-term climatic changes and the larch radial growth on the northern Middle
891 Siberia and the Northeastern Yakutia in the Late Holocene. Abs. PHD Diss, V.N.
892 Sukachev Institute of Forest, Krasnoyarsk, 2003.
- 893 Sidorova, O.V., Naurzbaev, M.M., Vaganov, E.A.: Response of tree-ring chronologies growing
894 on the Northern Eurasia to powerful volcanic eruptions. Problems of ecological moni-
895 toring and ecosystem modeling, XX, 60-72, 2005.
- 896 Sidorova, O.V., Saurer, M., Myglan, V.S., Eichler, A., Schwikowski, M., Kirilyanov, A.V.,
897 Bryukhanova, M.V., Gerasimova, O.V., Kalugin, I., Daryin, A., Siegwolf, R.: A
898 multi-proxy approach for revealing recent climatic changes in the Russian Altai. Cli-
899 mate Dynamics, 38 (1-2), 175–188, 2011.
- 900 Sidorova, O.V., Siegwolf, R., Myglan, V.S., Loader, N.J., Helle, G., Saurer, M.: The applica-
901 tion of tree-rings and stable isotopes for reconstructions of climate conditions in the
902 Altai-Sayan Mountain region. Climatic Changes, doi: 10.1007/s10584-013-0805-5,
903 2012.
- 904 Sidorova, O.V., Siegwolf, R., Saurer, M., Naurzbaev, M., Shashkin, A.V., Vaganov, E.A.: Spa-
905 tial patterns of climatic changes in the Eurasian north reflected in Siberian larch tree-
906 ring parameters and stable isotopes. Global Change Biology, doi: 10.1111/j.1365-
907 2486.2009.02008.x, 16, 1003-1018, 2010.
- 908 Sidorova, O.V., Siegwolf, R.T.W., Saurer, M., Naurzbaev, M.M., Vaganov, E.A.: Isotopic
909 composition ($\delta^{13}\text{C}$, $\delta^{18}\text{O}$) in Siberian tree-ring chronology. Geophysical research
910 Biogeosciences. 113, 1-13, 2008.
- 911 Sigl, M., Winstrup, M., McConnell, J.R.: Timing and climate forcing of volcanic eruptions for
912 the past 2500 years. Nature. 523, 543-549. doi:10.1038/nature14565, 2015.

- 913 Sprenger, M., Tetzlaff, D., Buttle, J. M., Laudon, H., Leister, H., Mitchell, C., Snelgrove, J.,
914 Weiler, M., Soulsby, C.: Measuring and modelling stable isotopes of mobile and bulk
915 soil water, *Vadose Zone Journal*, <https://doi.org/10.2136/vzj2017.08.0149>, 20, 2017.
- 916 Sternberg, L.S.O.: Oxygen stable isotope ratios of tree-ring cellulose: The next phase of un-
917 derstanding. *New Phytologist*. 181 (3), 553-562, 2009.
- 918 Stirzaker, D.: *Elementary Probability density functions*. Cambridge. Sec. Ed. 538 p, 2003.
- 919 Stoffel, M., Khodri, M., Corona, C., Guillet, S., Poulain, V., Bekki, S., Guiot, J., Luckman,
920 B.H., Oppenheimer, C., Lebas, N., Beniston, M., Masson-Delmotte, V.: Estimates of
921 volcanic-induced cooling in the Northern Hemisphere over the past 1,500 years. *Nature*
922 *Geoscience*. 8, 784–788, 2015.
- 923 Stothers, R.B.: Climatic and Demographic Consequences of the Massive Volcanic Eruption of
924 1258. *Climatic Change*. 45, 361-374, 2000.
- 925 Stothers, R.B.: Mystery cloud of AD 536. *Nature*. 307, 344-345, doi:10.1038/307344a0, 1984.
- 926 Sugimoto, A., Yanagisawa, N., Fujita, N., Maximov, T.C.: Importance of permafrost as a
927 source of water for plants in east Siberian taiga. *Ecological Research*. 17 (4), 493-
928 503, 2002.
- 929 Toohey, M., Sigl, M.: Volcanic stratospheric sulphur injections and aerosol optical depth
930 from 500 BCE to 1900 CE. *Earth System Science Data*. doi:10.5194/essd-9-809-
931 2017, 2017.
- 932 Vargas, A. I., Schaffer, B., Yuhong, L. Sternberg, L.S.: Testing plant use of mobile vs immo-
933 bile soil water sources using stable isotope experiments. *New Phytologist*. 215, 582–
934 594, doi: 10.1111/nph.14616, 2017.
- 935 Vaganov, E.A., Hughes, M.K., Kirilyanov, A.K., Schweingruber, F.H., Silkin, P.P.: Influence
936 of snowfall and melt timing on tree growth in subarctic Eurasia. *Nature*. 400, 149-151,
937 1999.

- 938 Vaganov, E.A., Hughes, M.K., Shashkin, A.V.: Growth dynamics of conifer tree rings. Springer
939 Verlag, Berlin., pp. 353, 2006.
- 940 Wegmann, M., Brönnimann, S., Bhend, J., Franke, J., Folini, D., Wild, M., Luterbacher, J.:
941 Volcanic influence on European summer precipitation through monsoons: Possible
942 cause for “years without summer”. AMS, doi.org/10.1175/JCLI-D-13-00524.1, 2014.
- 943 Wigley, T.M.L., Briffa, K.R., Jones, P.D.: On the Average Value of Correlated Time Series,
944 with Applications in Dendroclimatology and Hydrometeorology. *Journal of Climate*
945 and Applied Meteorology. 23 (2), 201-213, doi:10.1175/15200450(1984)023.0201,
946 1984.
- 947 Wiles, G.C., D’Arrigo, R.D., Barclay, D., Wilson, R.S., Jarvis, S.K., Vargo, L., Frank, D.: Sur-
948 face air temperature variability reconstructed with tree rings for the Gulf of Alaska
949 over the past 1200 years. *The Holocene*. 6, 2014. 10.1177/0959683613516815.
- 950 Wilson, R.J.S., Anchukaitis, K., Briffa, K. et al.: Last millennium Northern Hemisphere sum-
951 mer temperatures from tree rings. Part I: the long-term context. *Quaternary Science*
952 *Review*. 134, 1–18, 2016.
- 953 Zielinski, G.A., Mayewski, P.A., Meeker, L.D., Whitlow, S., Twickler, M.S., Morrison, M.,
954 Meese, D.A., Gow A.J., Alley, R.B.: Record of volcanism since 7000 BC from the
955 GISP2 Greenland ice core implications for the volcano-climate system. *Science*. 264
956 (5161), 948-952, 1994.